**SHORT COMMUNICATION**

# Enrichment of aluminium in the near-surface region of natural quartzite rock after aluminium exposure

Klaus-Jürgen Hüenger<sup>1</sup> | Mario Kositz<sup>1</sup> | Matti Danneberg<sup>1</sup> | Jörg Radnik<sup>2</sup>

<sup>1</sup>Chair of Building Materials and Building Chemistry, Brandenburg University of Technology Cottbus-Senftenberg, Cottbus, Germany

<sup>2</sup>Division 6.1 "Surface Analysis and Interfacial Chemistry", Federal Institute for Materials Research and Testing (BAM), Berlin, Germany

**Correspondence**

Radnik, Jörg, Division 6.1 "Surface Analysis and Interfacial Chemistry", Federal Institute for Materials Research and Testing (BAM), Berlin, Germany.

Email: joerg.radnik@bam.de

Alkali-silica reaction (ASR) is an ongoing problem that causes damage to concrete constructions and reduces their durability. Therefore, minimizing this undesired reaction is of great interest for both safety and economic reasons. Additives containing high aluminium content are very effective in reducing the release of silica and enhancing the durability of concrete; however, the mechanism for this effect is still under discussion. In this study, an enrichment of aluminium in the near-surface region was observed for natural quartzite rock after storage in Al (OH)<sub>3</sub> and metakaolin as aluminium sources, from which we conclude that the formation of aluminosilicate sheets of a few nanometres inhibits the silica release; this hypothesis is supported by high-resolution spectra of Al 2p, Si 2p and O 1s.

**KEYWORDS**

alkali-silica reaction, quartzite rock, X-ray photoelectron spectroscopy

## 1 | INTRODUCTION

Interactions between two or more phases are the basics of modern construction materials. Such interactions mainly occur through surface contact of the various phases of multicomponent systems. Therefore, the knowledge of surface properties is crucial for an understanding of these interactions.

Concrete is such a multicomponent system, consisting of the binder cement stone together with aggregates that are distributed throughout the matrix. Here, interactions between the binder and the aggregates are of great importance for achieving a dense structure and thus good strength properties.<sup>1</sup> On the other hand, surface properties of aggregates are responsible also for damaging reactions, which can lead to a destruction of the entire concrete structure<sup>2</sup> through reactions such as the alkali-silica reaction (ASR), which influences the durability of concrete; inhibiting this reaction is therefore an economically important goal.<sup>3</sup> One possibility to inhibit the ASR is to add so-called supplementary cementing materials (SCMs) to the concrete mixture, which are high-aluminium content additives that are very effective and have a great importance for concrete

technology.<sup>4</sup> However, the inhibition mechanisms of SCMs are not completely understood. One effect arising from incorporation of SCMs is that the dissolution rate of silica from aggregates is strongly reduced by the presence of aluminium. This decreased release of silica can reduce the formation of undesired reaction products that are believed to lead to concrete damage. Changes of the surface properties of the concrete by soluble aluminium were discussed as one reason for this behaviour.

However, the idea that dissolved aluminium in alkaline solutions affects the silica release process is not new; Labrid<sup>5</sup> reported an influence on silica dissolution in dissolution experiments of fine-grained sand with and without aluminium. Bickmore et al<sup>6</sup> postulated that the coadsorption of Al (OH)<sub>4</sub><sup>-</sup> and Na<sup>+</sup> on silanol sites passivates the surrounding quartz surface. Chappex and Scrivener<sup>7</sup> investigated the changes of silica surface areas by microscopic methods and could find less dissolution pits in the areas treated with an aluminium supply. For these investigations, amorphous silica (silica glass) was used. The silica substrate was split into four quarters, and each of the quarters has been treated differently. Chappex and Scrivener<sup>8</sup> described results of X-ray photoelectron

This is an open access article under the terms of the Creative Commons Attribution License, which permits use, distribution and reproduction in any medium, provided the original work is properly cited.

© 2020 The Authors. Surface and Interface Analysis published by John Wiley & Sons Ltd



**FIGURE 1** Thick section samples after alkali attack (KOH), without (left) and with (right) exposure to aluminium solution

spectroscopy (XPS) investigations with such glass materials and concluded that aluminium was incorporated into the silica framework at reactive sites and decreased the interfacial free energy, which slowed down the silica dissolution. It must be noted that differences on the surfaces with and without Al influence are visible with naked eye (see Figure 1), but only XPS was able to detect a very thin aluminium-containing layer on the surface of the silica glass.

Huenger<sup>9</sup> and Huenger et al<sup>10</sup> described a similar influence of aluminium on the dissolution of silica in natural rocks for the first time in which greywacke grains showed a similar behaviour to silica glass, but an understanding of the mechanism with natural rocks could not be elucidated.

The structure and the thickness of the aluminium-enriched surface regions to such natural rocks is still unknown. One possibility is an aluminium layer that is analogous to clay or mica minerals; alternatively, an aluminosilicate layer may be formed in the near-surface region of the grains of the natural rock. Infrared (IR) or Raman spectroscopy failed to solve this problem because of their insufficient surface sensitivity. The same is valid for X-ray diffraction, and with grazing incidence, the natural stone surfaces are not flat enough for reliable measurements. First results were demonstrated in Huenger et al.<sup>11,12</sup> In this study, we discuss how XPS can be used to gain deeper insights into the structure of the near-surface region of natural rocks after aluminium exposure.

## 2 | EXPERIMENTAL

### 2.1 | Materials

Dissolution experiments were performed with sections of quartzite grains, with a thickness of approximately 2 mm and a diameter corresponding to the original sizes of the grains used in concrete (here, 8–16 mm). Quartzite is a metamorphic rock consisting of 98 wt.-% quartz and approximately 2 wt.-% muscovite. Such samples were stored in highly alkaline KOH solutions with and without the presence of aluminium in the solution. Figure 1 shows a typical sample.

The alkaline solution had a concentration of 0.1 M, and the temperature of the solution was 80°C. As Al-providers, Al(OH)<sub>3</sub> and metakaolin were used. These powdery materials were added to the alkaline solution in which the quartzite samples stored. The duration

of storage was up to 14 days for dissolution experiments and up to 20 days for XPS investigations.

Si-Al reference samples were prepared by precipitating an aluminosilicate; sodium aluminate was added to a saturated potassium water glass solution to give a Si/Al ratio of 2.24. One sample was prepared at 20°C, and the other sample was warmed up at 80°C.

### 2.2 | Characterization

The XPS investigations were performed with an AXIS Ultra DLD photoelectron spectrometer (Kratos Analytical, Manchester, UK) with monochromatic Al K $\alpha$  radiation ( $E = 1,486.6$  eV). The pressure was kept below  $1 \times 10^{-8}$  mbar. The electron emission angle was 0°, and the source-to-analyser angle was 60°. The binding energy scale of the instrument was calibrated following a Kratos Analytical procedure that uses ISO 15472 binding energy data.<sup>13</sup> Spectra were taken by setting the instrument to the hybrid lens mode and the slot mode with a  $300 \times 700 \mu\text{m}^2$  analysis area. All spectra were recorded in the fixed analyser transmission (FAT) mode, and the charge neutralizer was used. The binding energies were referenced to the C 1s peak of aliphatic carbon at 285.0 eV. Before determining the peak area and fitting, the background were subtracted using a modified Toogaard background.<sup>14</sup> For the quantification, the survey spectra obtained with a pass energy of 80 eV were used. The peak intensities were corrected with the appropriate Scofield factors, the inelastic mean free path and the intensity response function of the instrument. The maximum relative uncertainty for the composition is  $\pm 10$  at%. The chemical species were determined with fits of the peaks measured with high resolution (pass energy of 20 eV). For the fits sum, Gaussian–Lorentzian profiles were used.<sup>15</sup> The binding energy has an uncertainty of  $\pm 0.2$  eV.

The sputtering experiments for depth profiling were performed with Quantum 2000 scanning ESCA microprobe (Physical Electronics, Chanhassan, MN, USA). As a radiation source, monochromatic Al K $\alpha$  radiation ( $E = 1486.6$  eV) was used. A monoatomic Ar sputter gun with a sputter rate of 1 nm/min (calibrated for SiO<sub>2</sub>) was used. High-resolution spectra with an energy step of 0.2 eV for the following peaks were detected: C 1s, O 1s, Si 2p, Al 2p, K 2p, Mg 2s and Fe 2p.

### 3 | RESULTS

#### 3.1 | Solubility experiments

Solubility experiments were performed with in KOH and in presence of metakaolin or Al (OH)<sub>3</sub> as Al sources. The effect of Al on the reduction of the silica-releasing rate can be demonstrated very well using Al (OH)<sub>3</sub> because of its Si-free composition. The results are shown in Figure 2. Figure 2A shows the solubility of quartzite grains prepared as thick section sample over a 14-day period. With approximately 90 mg/L, a detectable amount of silica can be found in the alkaline solution after 14 days of alkali attack, whereas the Al concentration is near zero because a very small amount of muscovite does not provide any measurable contribution to the Al release. With the presence of Al (OH)<sub>3</sub> (Figure 2B) in the alkaline solution, only the dissolution curves of the pure Al-provider material can be measured, whereas the measured silica concentration is very low.

To control the mechanism of aluminium exposed on the surface of the quartzite grains, solubility experiments were performed a second time. After aluminium exposure, the so-prepared samples were

stored in an alkaline 0.1-M KOH solution, with the results shown in Figure 2C. It can be seen that the amount of soluble silica, which comes from the quartzite grain, is reduced from 90 mg/L to approximately 60 mg/L. Important is that the Al concentration is near zero in this experiment, which means that the reduction of silica is not caused by an aluminosilicate formation precipitation process in the solution. Due to the fact that many analytical methods failed so far [Grazing Incidence X-ray diffraction (GI-XRD), Fourier transform infrared spectroscopy (FTIR)], the XPS method was selected to investigate this assumed thin layer on the surface of the quartzite.

#### 3.2 | XPS analysis

XPS analysis were performed on the pristine material and both Al (OH)<sub>3</sub>- and metakaolin-coated samples. Figure 3A shows the evaluation of the Al/Si ratio in the near-surface region after 7 and 20 days of exposure of pristine quartzite in a KOH solution with metakaolin as the Al source. Al was deposited on the surface, with the ratio after 7 days similar to after 20 days. This means that the deposition of Al

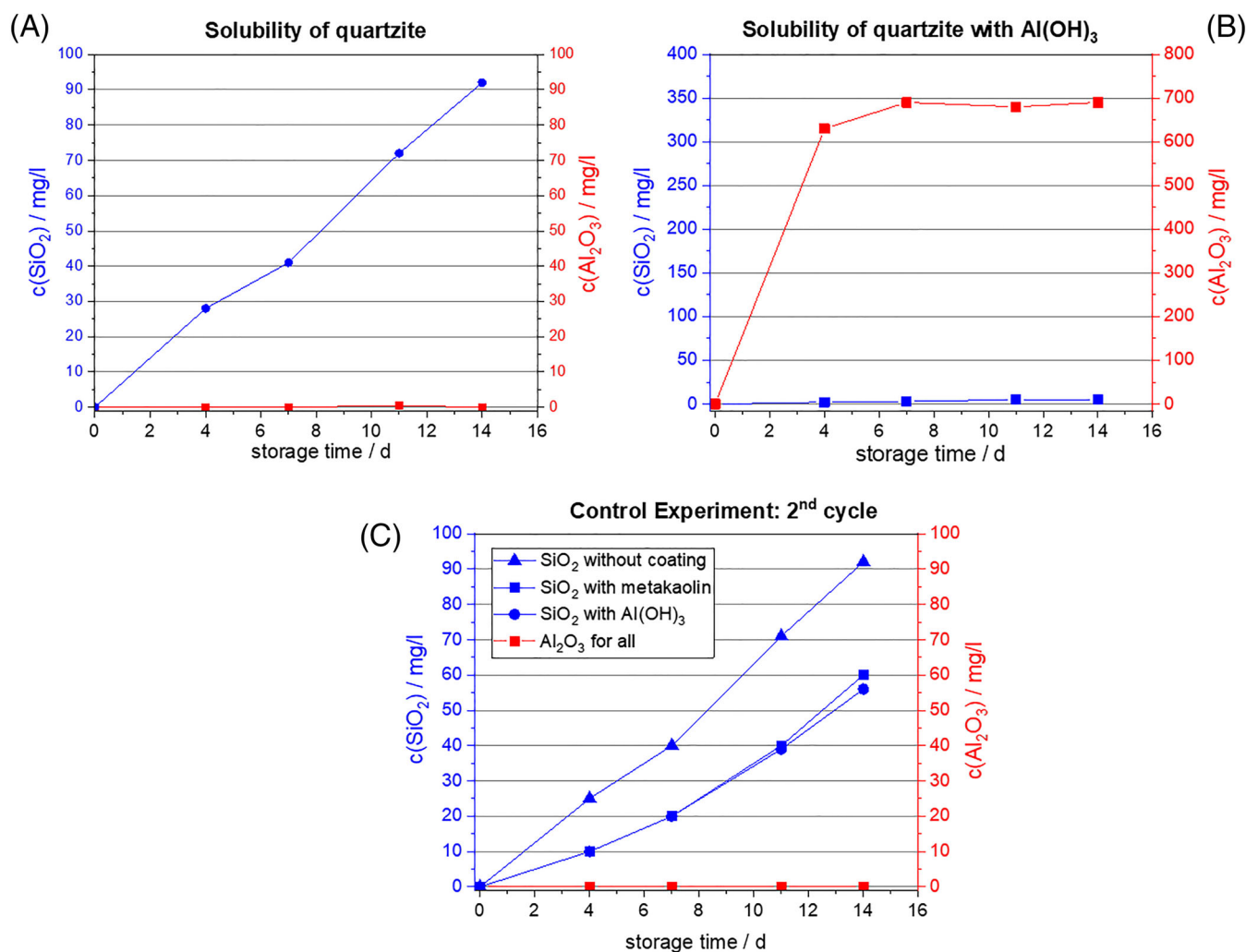


**FIGURE 2** Dissolution curves of Si and Al in the KOH of pure quartzite (A), in the presence of Al (OH)<sub>3</sub> (B) and in the second cycle (C)

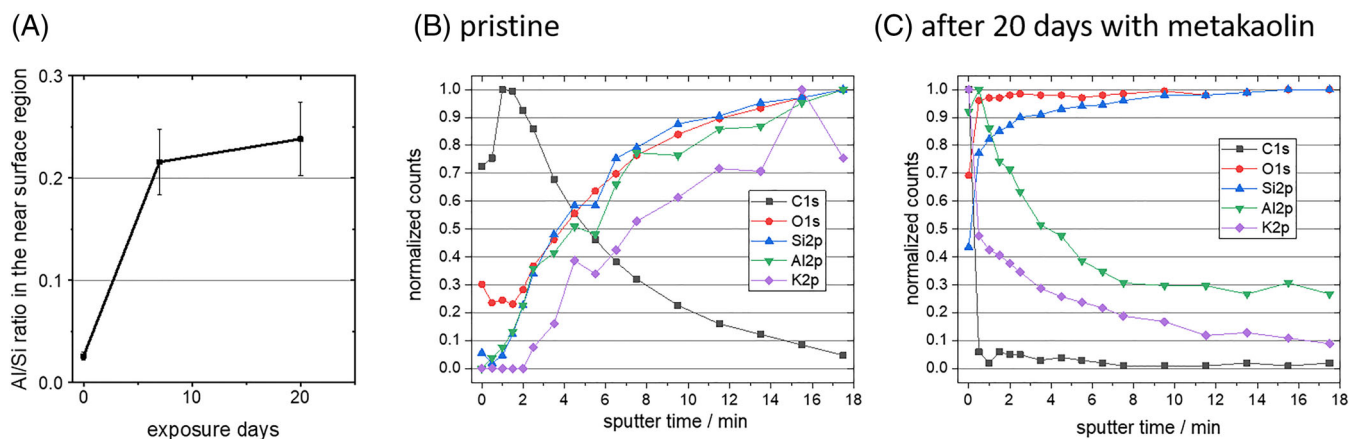


**FIGURE 3** Evaluation of the Al/Si ratio during 20 days of treatment in KOH with metakaolin (A) and depth profiles by sputtering of pristine quartzite (B) and the treated quartzite (C)

was mostly completed after 1 week of coating. The corresponding XPS spectra are shown in Figure S1.

Depth profile investigations were also made to determine the thickness of this Al-containing layer with 8–10 nm (Figure 3B,C). The calibration was done with a quartz crystal, where 1-min sputtering represents 1-nm abrasive depth. The intensities of each data point are normalized to the maximum intensity of the respective peak.

Figure 3B shows the depth profile of the pristine quartzite. In the outermost layer, carbon is present with decreasing intensity and increasing depth. At layers deeper than 15 nm, the sample was carbon-free. At the outermost first nanometres, only oxygen was detected next to carbon. This result can be explained with a relatively thick film of adventitious carbon. More important for our study is that the Si and Al concentrations increase in parallel with increasing sputter time. An enrichment of one of the components cannot be observed. In contrast, for the sample treated with metakaolin for 20 days, the Al content decreases with increasing depth, whereas the Si content increases (Figure 3C). An enrichment of Al at the outer 10 nm was observed. For carbon, a thin layer of about 1 nm was observed typical for adventitious carbon. Potassium was also concentrated in the near-surface region because of the storage in KOH solution.

To obtain further insights into the chemical nature of the Al- and Si-containing compounds, high-resolution XPS measurements were performed to determine the binding energies of Si 2p, Al 2p and O1s photoelectrons (Figure 4). Table 1 summarizes the results. For these experiments, both Al (OH)<sub>3</sub> and metakaolin as Al sources were used. The aim of these measurements was to examine the formation of aluminosilicates; therefore, two aluminosilicate samples were measured as references.

As expected, for both treated reference samples, a higher amount of Al was found (see last two lines in Table 1). The low amount of Al in the pristine quartzite sample can be explained by trace amounts of muscovite. The treated samples were stored in KOH with and without the presence of the Al sources, Al (OH)<sub>3</sub> and metakaolin, respectively. Although differences are visible (see

Figure 1), the XPS results look very similar on the first view. The presence of the Al-sources influences the Al/Si ratio (on average from 0.02 for pristine quartz to 0.10 for KOH to 0.21 for KOH/Al (OH)<sub>3</sub> and 0.15 for KOH/metakaolin). These data confirm the investigation results described earlier. With the treated samples, a small shoulder of the O1s peak at 530.8 eV was detected with a relative intensity below 5% for the KOH and KOH + Al (OH)<sub>3</sub> and ca. 12% for the sample treated with metakaolin. The binding energy corresponds to pure Al<sub>2</sub>O<sub>3</sub>,<sup>16</sup> but such a shoulder was also detected by Chappex and Scrivener,<sup>8</sup> where it was explained by the incorporation of aluminium on the surface of silica. The depth profile of the metakaolin treated sample (Figure 3C) supports this theory. Another possible explanation for this shoulder is pure Al<sub>2</sub>O<sub>3</sub> or Al (OH)<sub>6</sub> originating from the muscovite as a mineral part of the quartzite grains.

The influence of the formation of Al-O-Si bonds on the binding energies of O 1s, Si 2p and Al 2p photoelectrons was investigated with both Si-Al reference samples, one as prepared at room temperature and the other one warmed up at 80°C. For these reference samples, respective Al/Si ratios of 0.53 and 0.58 were determined. The binding energy of the Si 2p photoelectrons was 102.6 eV for the reference without any warming and 102.3 eV for the sample after warming. It may be suggested that the moderate warming led to a further formation of Al-O-Si bonds. These results show that the influence of the formation of the Al-O-Si bonds on the Si 2p binding energies was much more pronounced than on the Al 2p energies. The same decrease of the binding energy found for the Si 2p photoelectrons was also observed for the O 1s main peak. Thus, Si 2p or O 1s seems to be the suitable probes for the determination of aluminosilicates. For the determination of the binding energies of the oxides, it must be considered that the O 1s oxide peak can be overlapped with other oxygen species, for example, hydroxide or oxygen from organic components. Alternatively, the difference  $\Delta$  between the Si 2p and the Al 2p peaks can be used for the determination of Al-O-Si bonds. This approach proposed by Herreros et al<sup>17</sup> and Klinowski and Barr<sup>18</sup> uses the observation that the

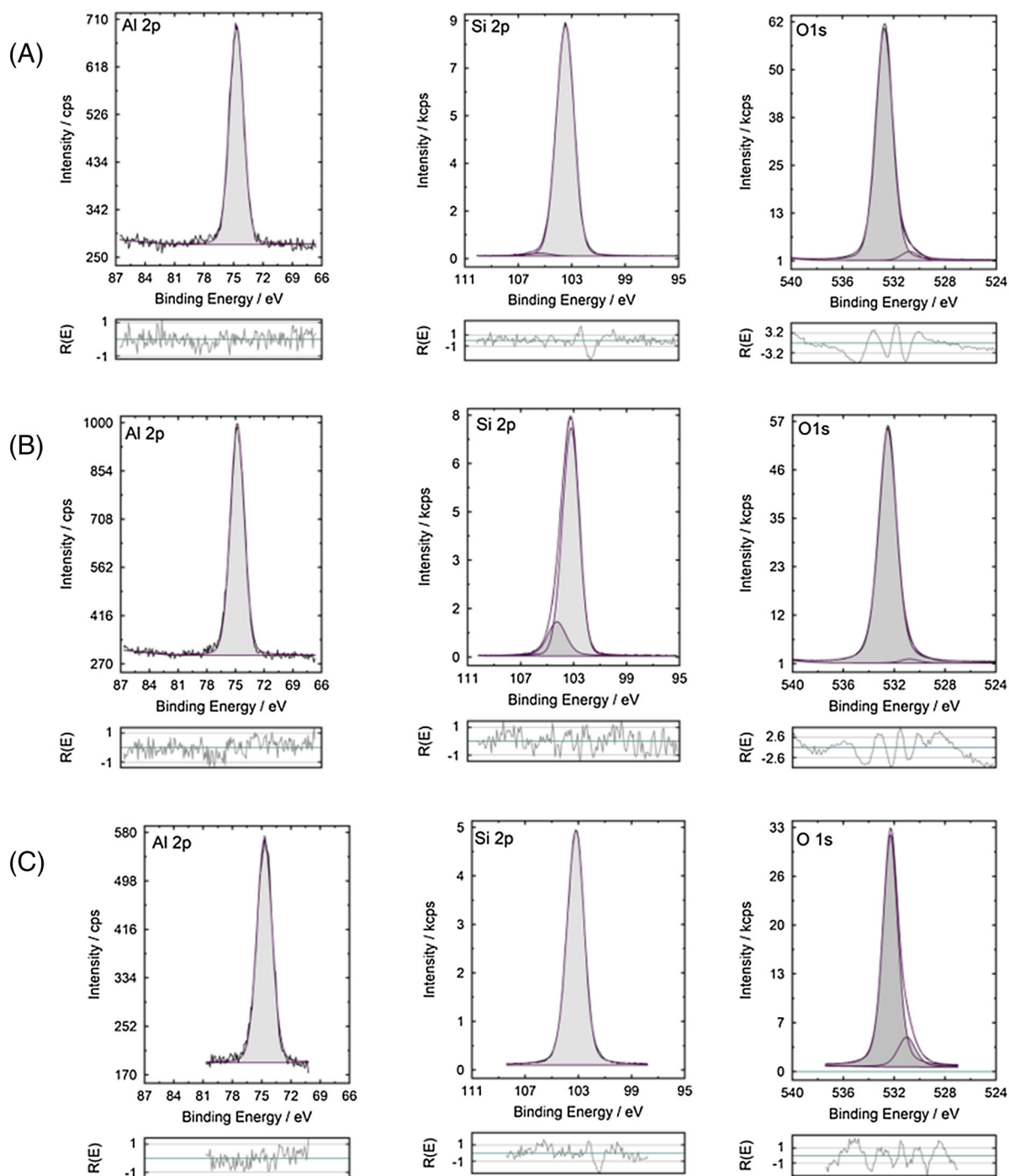


**FIGURE 4** High-resolution spectra of Al 2p, Si 2p and O 1s photoelectrons obtained from the samples stored in KOH without any Al source (A), with Al (OH)<sub>3</sub> (B) and with metakaolin (C) as Al sources

binding energies of Si 2p photoelectrons are more influenced by the formation of Al-O-Si bonds than the Al 2p photoelectrons, which corresponds to our results described above. An advantage of this approach is that charging effects or problems with internal binding energy referencing, which are discussed in the literature in detail,<sup>19</sup> can be excluded, but the effect on  $\Delta$  is rather small even for the reference samples with a value of 0.5 eV. For the sample stored in KOH alone, no changes for  $\Delta$  compared with the pristine sample

were observed, whereas for the Al-coated samples slight changes of 0.2 or 0.3 eV were observed. These slight changes are within the uncertainty range of the binding energy; otherwise, they correspond to the Al amount found in these samples. In summary, the exact determination of the binding energies with as low as possible uncertainty is crucial for the reliable determination of aluminosilicate concentrations. The approach involving minimizing charging effects seems to be potentially the best way to solve this problem.

**TABLE 1** Binding energies of Si 2p and Al 2p and differences between  $E_B$ 

Sample	Al/Si ratio	$E_B^F$ (Si 2p) /eV	$E_B^F$ (Al 2p) /eV	$\Delta$ /eV $\Delta = E_B^F$ (Si 2p) – $E_B^F$ (Al 2p)	$E_B^F$ (O 1s) /eV
Quartzite/pristine	0.02	103.4	74.7	28.7	532.8
Stored in KOH	0.08	103.3	74.6	28.7	532.7
KOH/Al (OH) <sub>3</sub>	0.21	103.0	74.7	28.3	532.5
KOH/metakaolin	0.15	103.0	74.6	28.4	532.3
Si-Al-reference	0.53	102.4	74.3	28.1	531.5
Si-Al-warmed up	0.58	102.1	74.0	28.1	531.6

Note. The relative uncertainty range for the ratio is  $\pm 15\%$ , for the binding energies including  $\Delta \pm 0.2$  eV.

## 4 | CONCLUSION

Based on solubility investigations, it can be concluded that the SiO<sub>2</sub> solubility of aggregates can be strongly reduced in the presence of Al (OH)<sub>3</sub> or metakaolin (MK). After alkali attack, an additional 40% decrease in the solubility of aggregates prepared with Al-containing SCMs on the surfaces can be measured. For such treated samples, only with XPS was it possible to find evidences for an aluminium enrichment in the near-surface region of the outermost 10 nm. Storage in KOH lead to a slight enrichment of Al in this region originating from Al<sub>2</sub>O<sub>3</sub> or Al (OH)<sub>4</sub><sup>−</sup> particles deposited on or incorporated in the quartzite. As expected, presence of an Al source like Al (OH)<sub>3</sub> or metakaolin lead to more pronounced enrichment, with two until three times higher amount of Al in the near-surface region. Depth profiling with sputtering confirmed this Al enrichment. High-resolution XPS investigations suggested the incorporation of aluminium ions in the silica surface and the formation of the aluminosilicate structures, but further efforts are necessary for clear evidence of such structures. These aluminosilicate sheets can explain the inhibitory effect of Al-containing SCMs on the dissolution of SiO<sub>2</sub>. All these investigations were done at surface areas of natural stones prepared and polished in the same way as for light microscopy investigations. Due to the thin layer of approximately 10 nm, other methods such as Raman spectroscopy or grazing-incidence XRD failed with their significantly lower surface sensitivity. The approach used in this study offers new possibilities in the understanding of ASR inhibition.

## ACKNOWLEDGEMENTS

The authors thank Mr Mike Mühlstädt (Friedrich-Schiller-University, Jena) for performing the sputtering experiments and Mr Jörg-Manfred Stockmann (BAM, Berlin) for performing XPS measurements. Open access funding enabled and organized by Projekt DEAL.

## ORCID

Jörg Radnik  <https://orcid.org/0000-0003-0302-6815>

## REFERENCES

- Weber R. *Good Concrete-Advices for the Right Concrete Production*. Verlag Bau u. Technik, ISBN 978-3-7640-0586-3 (in German); 2014.
- Stark J, Wicht B. *Durability of Concrete*. Springer Vieweg, ISBN 978-3-642-35277-5 (in German); 2013.
- Rieke C. Betonkrebs frisst Steuergelder auf. 2017; see <https://www.n-tv.de/wirtschaft/Betonkrebs-frisst-Steuergelder-auf-article19912778.html>. Accessed September 01, 2020.
- Thomas M. The effect of supplementary cementing materials on alkali-silica reaction: a review. *Cem Concr Res*. 2010;41:1224-1231.
- Labrid J. Modelling of high pH sandstone dissolution. *J Can Petrol Technol*. 1991;30:67-74.
- Bickmore BR, Nagy KL, Gray AK, Brinkerhoff AR. The effect of Al (OH)<sub>4</sub><sup>−</sup> on the dissolution rate of quartz. *Geochim Cosmochim Acta*. 2006;70:290-305.
- Chappex T, Scrivener K. The influence on aluminium on the dissolution of amorphous silica and its relation to alkali silica reaction. *Cem Concr Res*. 2012;42:1513-1523.
- Chappex T, Scrivener K. The effect of aluminum in solution on the dissolution of amorphous silica and its relation to cementitious systems. *J Am Ceram Soc*. 2013;96:592-597.
- Huenger KJ. The contribution of quartz and the role of aluminum for understanding the AAR with greywacke. *Cem Concr Res*. 2007;37:1193-1205.
- Huenger KJ, Kronemann J, Huebert C, Scholz Y. On the mechanism of ASR inhibition by Si and Al containing SCMs. In: Gupta PR, Gupta P, eds. *Supplementary Proceedings of the 13th International Conferences on Recent Advances in Concrete Technology and Sustainability Issues*. Ottawa, Canada, ISBN: 978-0-9916737-3-5; 2015: 437-446.
- Huenger KJ, Kositz M, Huenger M, Krey J, Muehlstaedt M. Surface coating of siliceous part of aggregate grains by alumina containing SCM's in alkaline solutions. In: Bernardes HM, Hasparyk NP, eds. *Proceedings of 15th International Conference on Alkali Aggregate Reaction in Concrete*. Sao Paulo, Brazil. ISBN: 2525-4189; 2016.
- Huenger KJ, Kositz M, Danneberg M, Radnik J. XPS investigations on quartzite surfaces of natural rock samples for proof of Al exposure. 27<sup>th</sup> Annual Conference of the German Crystallographic Society/*Zeitschrift für Kristallographie*. Supplement, 110, ISBN 978-3-11-065403-5, 2019.
- ISO. 15472:2010: surface chemical analysis—X-ray photoelectron spectrometers—calibration of energy scales, Geneva, 2010.
- Hesse R, Denecke R. Improved Tougaard calculation by introduction of fittable parameters for the inelastic electron scattering cross-section in the peak fit of photoelectron spectra with Unifit. *Surf Interface Anal*. 2011;43:1514-1526.
- Hesse R, Streubel P, Szargan R. Product or sum: comparative tests of Voigt, and product or sum Gaussian and Lorentzian functions in the fitting of synthetic Voigt-based s-ray photoelectron spectra. *Surf Interface Anal*. 2007;39:381-391.
- Moulder JF, Stickle WF, Sobol PE, Bomben KD. *Handbook of X-ray Photoelectron Spectroscopy*. Eden Prairie, MN: Perkin-Elmer Corp; 1992.

17. Herreros H, He H, Barr TL, Klinowski J. ESCA studies of framework silicates with the soladite structure: 1. comparison of purely siliceous sodalite and aluminosilicate soladite. *J Phys Chem.* 1994;98:1302-1305.
18. Klinowski J, Barr TL. NMR and ESCA chemical shifts in aluminosilicates: a critical discussion. *Acc Chem Res.* 1999;32:633-640.
19. Biino GG, Gröning P. X-ray photoelectron spectroscopy (XPS) used as a structural and chemical surface probe on aluminosilicate minerals. *Eur J Mineral.* 1998;10:423-437.

#### SUPPORTING INFORMATION

Additional supporting information may be found online in the Supporting Information section at the end of this article.

**How to cite this article:** Hüenger K-J, Kositz M, Danneberg M, Radnik J. Enrichment of aluminium in the near-surface region of natural quartzite rock after aluminium exposure. *Surf Interface Anal.* 2020;1-7. <https://doi.org/10.1002/sia.6918>